Supporting Information: Tunable Terahertz Hybrid Metal-Graphene Plasmons

Mohammad M. Jadidi,[*,†] Andrei B. Sushkov,[‡] Rachael L. Myers-Ward,[¶] Anthony K. Boyd,[¶] Kevin M. Daniels,[¶] D. Kurt Gaskill,[*,¶] Michael S. Fuhrer,[*,‡,§] H. Dennis Drew,[*,‡] and Thomas E. Murphy[*,†]

†*Institute for Research in Electronics & Applied Physics, University of Maryland, College Park, MD 20742, USA*

‡*Center for Nanophysics and Advanced Materials, University of Maryland, College Park, Maryland 20742, USA*

¶*US Naval Research Laboratory, Washington DC 20375, USA*

§*School of Physics, Monash University, 3800 Victoria, Australia*

E-mail: mmjadidi@umd.edu; kurt.gaskill@nrl.navy.mil; michael.fuhrer@monash.edu; hdrew@umd.edu; tem@umd.edu

S1 Plasmon Modes in Metal/Graphene Grating

Maxwell's equations are solved for the general case of plasmon modes in a graphene-metal array with period Λ under normal-incidence plane-wave excitation as shown in Figure S1. We employ the method described in[1] to obtain an integral equation for the $E(x)$, complex amplitude of the x-polarized electric field within the graphene channel,

$$E(x) = \frac{\beta_c}{\beta\left(1 + \frac{\beta_c}{2}\right)} E_{\text{in}} + \frac{\beta - \beta_c}{\beta\Lambda} \sum_{l=-\infty}^{\infty} \frac{e^{i2\pi l x/\Lambda}}{1 + i\frac{\kappa_l \beta_c}{2}} \int_{-w/2}^{w/2} E(x') e^{-i2\pi l x'/\Lambda} dx' \tag{S1}$$

where E_{in} denotes the complex amplitude of the normally-incident, x-polarized incident plane wave with free-space wavelength λ, and $\kappa_l^2 = [(l\lambda/\Lambda)^2 - 1]$. β and β_c represent the frequency-dependent (Drude) conductivity of the 2D material and contact, respectively, normalized to the free-space impedance,

$$\beta = \sigma(\omega)\frac{Z_0}{\sqrt{\epsilon}} \qquad , \qquad \beta_c = \sigma_c(\omega)\frac{Z_0}{\sqrt{\epsilon}}$$

where Z_0 ($= 377\ \Omega$) is the wave impedance in vacuum. The contact conductivity σ_c is either zero, to model isolated graphene ribbons without contacts, or infinity to model a perfect electrical conducting boundary, or more generally it can describe the Drude response of an arbitrary conductive contact. The sheet conductivity of the metal was estimated from the bulk Drude conductivity, multiplied by the metal film thickness.

By Fourier-expanding the electric field in the graphene channel from $-w/2$ to $+w/2$,

$$E(x) = \sum_{n=0}^{\infty} E_n \cos(2\pi n x/w) \tag{S2}$$

the integral equation (S1) can be re-cast as a matrix equation,

$$\left[\frac{1+\delta_{0m}}{2}\delta_{mn} + \frac{(\beta_c-\beta)}{4\beta}\frac{w}{\Lambda}\sum_{l=-\infty}^{\infty}\frac{R_{mn}^{(l)}}{1+i\frac{\kappa_l\beta_c}{2}}\right]E_n = \delta_{m0}\frac{\beta_c}{\beta(1+\beta_c/2)}E_{\text{in}} \tag{S3}$$

where

$$R_{mn}^{(l)} \equiv [\text{sinc}(n\pi + l\pi w/\Lambda) + \text{sinc}(n\pi - l\pi w/\Lambda)] \\ \times [\text{sinc}(m\pi + l\pi w/\Lambda) + \text{sinc}(m\pi - l\pi w/\Lambda)] \tag{S4}$$

The Fourier components of the electric field can be obtained by numerically solving (S3). In practice, for smoothly-varying plasmon modes, only the lowest few Fourier components are needed to accurately approximate the field.

Then, from $E(x)$, the fractional absorbed power in the 2D material is computed as

$$A_G(\omega) = \frac{Z_0/\sqrt{\epsilon_0}}{2\Lambda|E_{\text{in}}|^2}\int_{-w/2}^{w/2}\text{Re}\Big\{J^*(x)E(x)dx\Big\} = \frac{\text{Re}\{\beta\}}{2\Lambda}\frac{1}{|E_{\text{in}}|^2}\int_{-w/2}^{w/2}|E(x)|^2dx \tag{S5}$$

S2 Equivalent Circuit Model

The optical response and plasmon resonance of the metal-graphene grating can be approximated from a two-port transmission line model shown in Figure S2(a). The resistance, inductance and capacitances appearing in this model are defined as:

$$R_G = \sigma_0^{-1} \tag{S6}$$

$$L_G = (\sigma_0\Gamma)^{-1} \tag{S7}$$

$$C_G = 2\epsilon_0\bar{\epsilon}\Lambda\ln[\sec(\pi w/2\Lambda)]/\pi \tag{S8}$$

$$C_M = 2\epsilon_0\bar{\epsilon}\Lambda\ln[\csc(\pi w/2\Lambda)]/\pi \tag{S9}$$

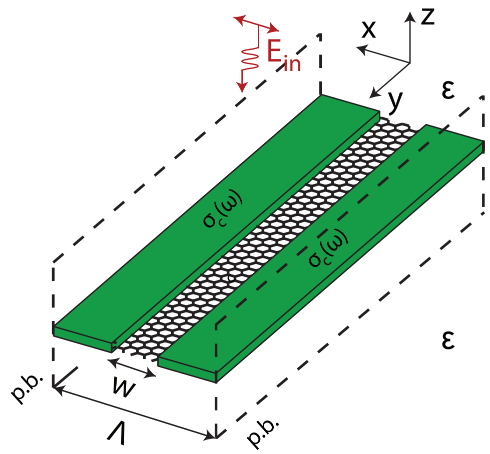

Figure S1: A unitcell of a periodic array (in x direction) of graphene-contact. Λ is the array period and w is the graphene channel width. ϵ is the dielectric constant of the surrounding material. $\sigma_c(\omega)$ is the contact conductivity. (p.b.: periodic boundary)

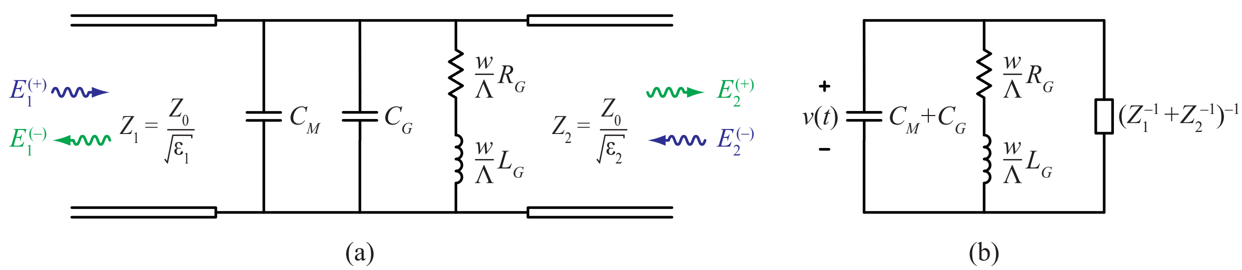

Figure S2: (a) Equivalent two-port transmission line model representing the sub-wavelength graphene-metal periodic structure. (b) Simplified circuit model when there are no input waves to the system, which is used to determine resonant (plasmon) frequency and damping rate.

and the incident and substrate regions are modeled as transmission lines with characteristic impedances of $Z_1 \equiv Z_0/\sqrt{\epsilon_1}$ and $Z_2 \equiv Z_0/\sqrt{\epsilon_2}$, respectively.

The graphene and contact capacitances can be combined into a single equivalent capacitance of

$$C = C_G + C_M = 2\epsilon_0\bar{\epsilon}\Lambda \ln(2\csc(\pi w/\Lambda))/\pi \tag{S10}$$

S2.1 Transmission, Reflection and Absorption

The relationship between the amplitudes of the incoming and outgoing wave amplitudes can be described by a scattering matrix,

$$\begin{bmatrix} E_1^{(-)} \\ E_2^{(+)} \end{bmatrix} = \begin{bmatrix} S_{11} & S_{12} \\ S_{21} & S_{22} \end{bmatrix} \begin{bmatrix} E_1^{(+)} \\ E_2^{(-)} \end{bmatrix} \tag{S11}$$

For the circuit model shown in S3(a), the scattering matrix is calculated to be:

$$\begin{bmatrix} S_{11} & S_{12} \\ S_{21} & S_{22} \end{bmatrix} = \frac{1}{Y_1 + Y_2 + Y(\omega)} \begin{bmatrix} Y_1 - Y_2 - Y(\omega) & 2Y_2 \\ 2Y_1 & Y_2 - Y_1 - Y(\omega) \end{bmatrix} \tag{S12}$$

where $Y_i = 1/Z_i$ and $Y(\omega)$ is the complex admittance of the combined resistor, capacitor and inductor,

$$Y(\omega) = \frac{\Lambda/w}{R_G - i\omega L_G} - i\omega C \tag{S13}$$

For waves incident from region 1, the reflection, transmission and absorption are calculated to be

$$R(\omega) = |S_{11}|^2 = \left| \frac{Y_1 - Y_2 - Y(\omega)}{Y_1 + Y_2 + Y(\omega)} \right|^2 \tag{S14}$$

$$T(\omega) = \frac{Y_2}{Y_1}|S_{21}|^2 = \frac{4Y_1Y_2}{|Y_1 + Y_2 + Y(\omega)|^2} \tag{S15}$$

$$A_G(\omega) = 1 - R(\omega) - T(\omega) = \frac{4Y_1 \operatorname{Re}\{Y(\omega)\}}{|Y_1 + Y_2 + Y(\omega)|^2} \tag{S16}$$

S2.2 Resonant Frequency and Linewidth

If there are no input waves applied to the system, the two transmission lines representing regions 1 and 2 may be simply replaced by their equivalent parallel impedance, which results in the simple second-order circuit shown in Figure S2(b). In this circuit model, the power dissipated in Z_1 and Z_2 represents the radiative loss into regions 1 and 2 respectively, while the power consumed in R_G gives the absorption in the two-dimensional material. Applying Kirchoff's laws, the voltage $v(t)$ is found to satisfy the following second-order homogeneous differential equation:

$$\ddot{v}(t) + \left[\frac{R_G}{L_G} + \frac{(Y_1 + Y_2)}{C}\right]\dot{v}(t) + \left[\frac{\Lambda/w}{L_G C} + \frac{R_G(Y_1 + Y_2)}{L_G C}\right]v(t) = 0 \tag{S17}$$

which describes a damped harmonic oscillator. In the limit of low-damping, the resonant frequency (or plasmon frequency) is

$$\omega_0 = \sqrt{\frac{\Lambda/w}{L_G C}} \tag{S18}$$

$$= e\sqrt{v_F\sqrt{\pi}/2\hbar}\sqrt{\frac{\sqrt{n}}{w\epsilon_0\bar{\epsilon}\ln[2\csc(\pi w/\Lambda)]}} \tag{S19}$$

The damping rate describes the linewidth of the plasmon resonance, which is found to be:

$$\Delta\omega = \frac{R_G}{L_G} + \frac{(Y_1 + Y_2)}{C} \tag{S20}$$

$$= \Gamma + \frac{\pi}{2\epsilon_0\bar{\epsilon}\Lambda \ln[2\csc(\pi w/\Lambda)]}\left(Z_1^{-1} + Z_2^{-1}\right) \tag{S21}$$

S2.3 Absorbed Power and Impedance Matching

In many applications, one wishes to optimize the power that is absorbed in the graphene layer, by appropriately designing or selecting the properties and dimensions of the grating and film. By maximizing the absorption (S16) with respect to the complex admittance $Y(\omega)$, one readily finds the optimal load admittance is

$$Y_{\text{opt}} = (Y_1 + Y_2)^* \tag{S22}$$

Since Y_1 and Y_2 are real numbers, (S22) implies that $Y(\omega)$ must be real, which occurs at an optimal frequency that is close to the resonant frequency,

$$\omega_{\text{opt}} = \sqrt{\frac{\Lambda/w}{L_G C} - \left(\frac{R_G}{L_G}\right)^2} \tag{S23}$$

$$Y(\omega_{\text{opt}}) = \frac{R_G}{L_G C} \tag{S24}$$

In this case, the condition for maximum power transfer to the graphene layer can be expressed as

$$\frac{R_G}{L_G} = \Gamma = (Y_1 + Y_2)/C \tag{S25}$$

which means that for maximum on-resonant absorption, the intrinsic material damping Γ is equal to the radiation damping.

Under these matched conditions, the lumped circuit may be regarded as impedance matching between two dissimilar media. The maximum fractional absorbed power is

$$A_{\max} = \frac{Y_1}{(Y_1 + Y_2)} \tag{S26}$$

S2.4 Circuit Model vs Finite Element Calculations

Figure S3 compares the transmission (T) and reflection (R) obtained from the full-wave finite element calculation (a and b) with the approximated values from circuit model (c and d). This figure exhibits close agreement between the results from circuit model (Figure S2a) and the exact solution for different grating periods.

S3 Geometrical Dependence

The equivalent circuit model predicts that the plasmon resonant frequency depends on the graphene channel width w and period Λ according to (S19). Apart from the weak logarithmic dependence on the duty cycle w/Λ, the resonant frequency is predicted to scale in proportion to $w^{-1/2}$, as for isolated graphene ribbons.[2,3] To confirm this scaling relation, we conducted a second set of reflection measurements using a graphene same that was fabricated with a narrower channel.

Figure S4 shows the normalized reflection measurement for metal-graphene gratings with two different graphene channel widths of $w = 350$ nm and 200 nm. For the same carrier density, the resonant frequency is seen to increase by approximately 30% ($= \sqrt{350 \text{ nm}/200 \text{ nm}}$) when the width is decreased, as predicted by (S19).

S4 Higher Order Plasmon modes

Beyond the fundamental mode that is considered in this letter, higher order plasmon modes also exist in the hybrid graphene-metal structure. Figure S5a shows the charge density profile

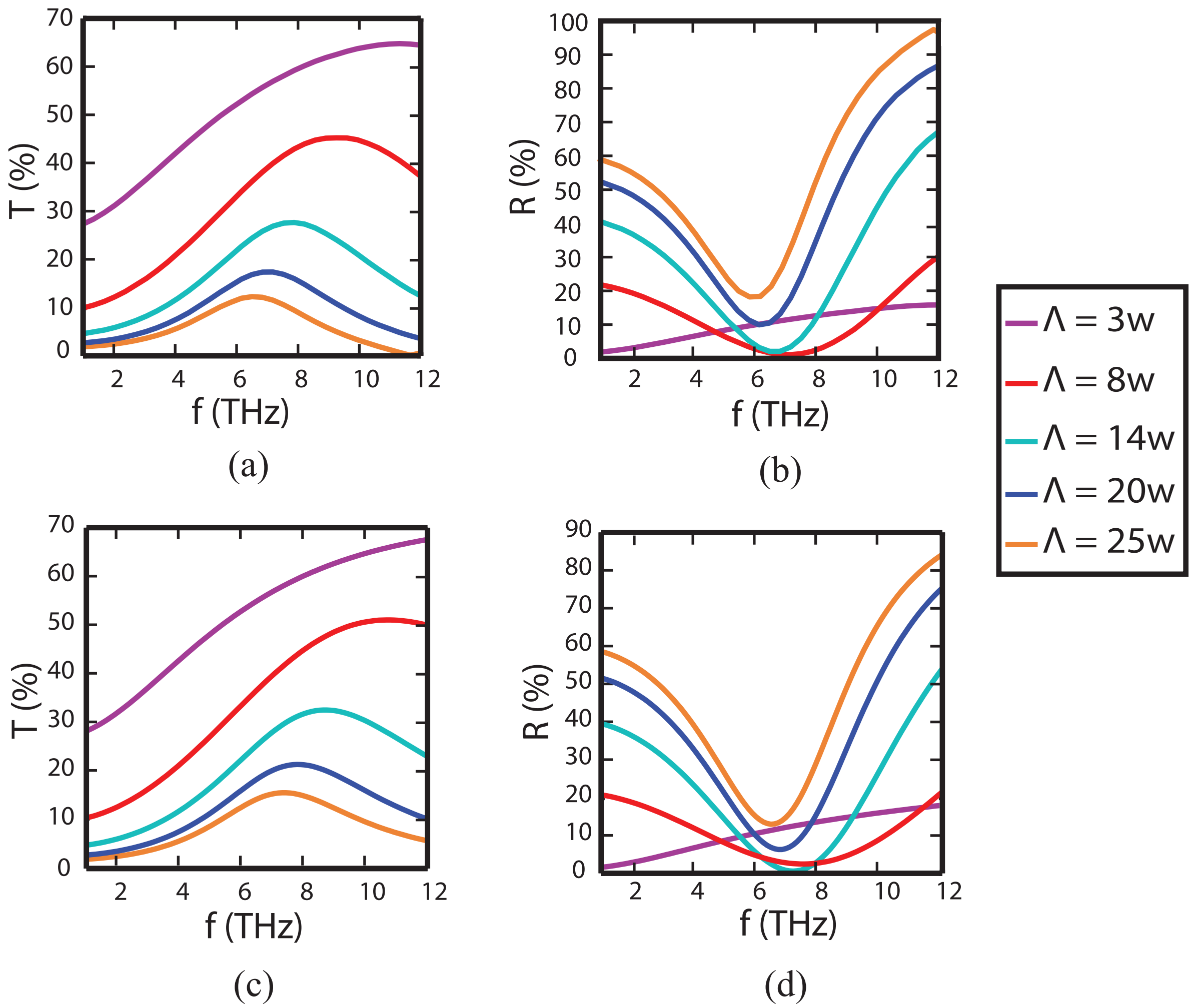

Figure S3: (a)/(b) transmission/reflection for different periods computed by full-wave finite element calculations. (c)/(d) transmission/reflection for different periods calculated by the circuit model showed in Figure S2a. $\epsilon_1 = 1$ (air), $\epsilon_2 = 9$ (SiC), $w = 0.35$ μm, $\mu = 1000$ cm^2/Vs, $n = 1.5 \times 10^{13}$ cm^{-2}

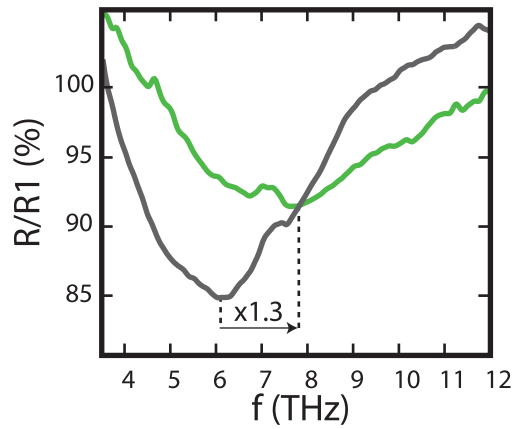

Figure S4: Comparison of measured normalized reflection for $w = 200$ nm, $\Lambda = 5$ μm (green curve), with $w = 350$ nm, $\Lambda = 7$ μm (gray curve) at the same carrier denisty $n = 10.3 \times 10^{12}$ cm^{-2}. Plasmon resonance is blue-shifted by about 30%.

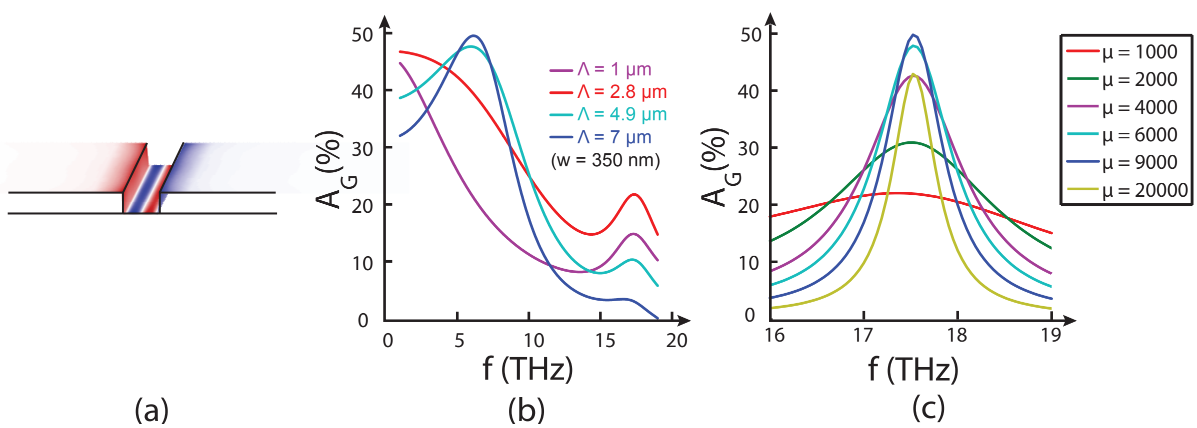

Figure S5: (a) Charge density profile at the 3rd plasmon mode frequency for metal-graphene structure. (b) Graphene absorption (A_G) under plane-wave excitation of metal-graphene gratings with different periods ($w = 350$ nm, $n = 1.5 \times 10^{13}$ cm^{-2}, $\mu = 1000$ cm^2 /Vs). The surrounding material was assumed to be uniform ($\epsilon_1 = \epsilon_2 = 5$). (c) Graphene absorption in metal-graphene gratings ($w = 350$ nm, $n = 1.5 \times 10^{13}$ cm^{-2}) with $\Lambda = 8w$ as a function of graphene mobility. The absorption is close to the maximum value (50%) for $\mu = 9000$ cm^{2}V^{-1}s^{-1}.

for the next dipole-active (third order) mode. Figure S5b is the same plot as in Fig. 1e but extended to show the behavior at higher frequencies. The third order mode appears as a small peak in the absorption around 17 THz. For the parameters chosen in this figure, the highest on-resonant absorption is obtained for $\Lambda = 8w = 2.8$ μm (red curve).

For the higher order modes, the equivalent circuit model Figure S2 can no longer be used to characterize the resonant frequency and radiative damping rate. We nonetheless expect that, as with the fundamental mode, optimal resonant absorption in the graphene can be attained when the radiative losses are matched to the graphene scattering rate. To confirm this principle, we varied the scattering rate Γ by changing the mobility μ. Figure S5c plots the calculated absorption for $\Lambda = 2.8$ μm for six different graphene mobilities ranging from 1000 to 20,000 $cm^2V^{-1}s^{-1}$. The absorption at the 3rd order peak approaches the theoretical maximum (50%) for graphene mobility of 9,000 $cm^2V^{-1}s^{-1}$. This demonstrates that, unlike most plasmonic structures in which higher order modes are weakly coupled to the incident plane-wave, the plasmon modes in the hybrid graphene-metal system can be efficiently excited by appropriately choosing the geometry of the metal contacts and graphene properties.

References

(1) Mikhailov, S. A.; Savostianova, N. A. *Phys. Rev. B* **2006**, *74*, 045325.

(2) Hwang, E. H.; Sarma, S. D. *Phys. Rev. B* **2007**, *75*, 205418.

(3) Ju, L.; Geng, B.; Horng, J.; Girit, C.; Martin, M.; Hao, Z.; Bechtel, H. A.; Liang, X.; Zettl, A.; Shen, Y. R.; Wang, F. *Nature Nanotech.* **2011**, *6*, 630–634.